Published in final edited form as:
J Mol Biol. 2008 June 6; 379(3): 579–588.

tRNA Integrity Is A Prerequisite for Rapid CCA Addition: Implication for Quality Control

Marcel Dupasquier[1], **Sangbumn Kim**[1], **Konstantine Halkidis**, **Howard Gamper**, and **Ya-Ming Hou**[*]
Thomas Jefferson University, Department of Biochemistry and Molecular Biology, 233 South 10th Street, Philadelphia, PA 19107

Summary

CCA addition to the 3′ end is an essential step in tRNA maturation. High-resolution crystal structures of the CCA enzymes reveal primary enzyme contact with the tRNA minihelix domain, consisting of the acceptor stem and T stem-loop. RNA and DNA minihelices are efficient substrates for CCA addition in steady-state kinetics. However, in contrast to structural models and steady-state experiments, we show here by single turnover kinetics that minihelices are insufficient substrates for the *E. coli* CCA enzyme, but that only the full-length tRNA is kinetically competent. Even a nick in the full-length tRNA backbone in the T loop, or as far away from the minihelix domain as in the anticodon loop, prevents efficient CCA addition. These results suggest a kinetic quality control provided by the CCA enzyme to inspect the integrity of the tRNA molecule and to discriminate against nicked or damaged species from further maturation.

Keywords

kinetic quality control; tRNA surveillance; single turnover kinetics

Many tRNA molecules must acquire the CCA sequence at their 3′ end as an essential step in the maturation process.[1] Also, tRNAs that are synthesized with the CCA sequence must be repaired in the event of CCA degradation by nucleases. The enzyme that catalyzes the synthesis and repair of the CCA sequence is ATP(CTP):tRNA nucleotidyl transferase (the CCA enzyme), which is present in all three domains of life and is essential for growth in organisms that lack the CCA sequence in their tRNA genes.[2] According to sequence motifs in the catalytic domains, the CCA enzymes are divided into two classes, where the archaeal enzymes are assigned to class I of the nucleotidyl transferase superfamily, while the bacterial and eukaryotic enzymes are assigned to class II.[3] Both classes of CCA enzymes use a single catalytic site to perform sequential nucleotide addition without copying a nucleic acid template, [4; 5; 6; 7; 8; 9; 10; 11] in contrast to template-dependent polynucleotide polymerases. The generally accepted model of the template-independent CCA addition assumes that both classes of CCA enzymes only bind to the acceptor-T stem loop of tRNA (the minihelix domain) for recognition.[6] This model is based on co-crystal structures of the class I *Archaeoglobus fulgidus* CCA enzyme (*Af*CCA) bound to a full-length tRNA (Fig.1A) and to minihelices.[9; 11] In these structures, the anticodon stem-loop (ASL) domain is projected outward while the minihelix

*Corresponding author; Telephone, 215-503-4480; Fax, 215-503-4954; Email, Ya-Ming.Hou@jefferson.edu.
[1]These authors contributed equally.

domains are in superimposable positions among various substrates and are held in fixed location by the enzyme. Consistent with footprint and biochemical analyses,[12; 13; 14] these structures reveal that the 3′ end of the minihelix domain refolds at each step of nucleotide addition to place the terminus at the active site. The minihelix domain is accommodated in an extended class I cleft that has a counterpart in class II enzymes with similar shape, charge, and dimensions.[6; 9] Indeed, tRNA minihelices are efficient substrates for both classes of CCA enzymes in steady-state kinetics.[15; 16; 17] However, we show here by fast kinetics of the class II *E. coli* CCA enzyme (*Ec*CCA) that the minihelix domain is insufficient to account for the kinetics of CCA addition, but that the full-length tRNA is necessary. Even a backbone break in ASL, distal from the acceptor end, causes a delay in CCA addition. These results suggest the possibility that the CCA addition serves to kinetically discriminate against nicked or damaged tRNA in the quality control of tRNA maturation.

Fast kinetics provides insights for understanding enzyme mechanisms that are unattainable from steady-state kinetics. The steady-state k_{cat} and K_m parameters are complex terms of all of the reactions occurring on the enzyme, such that individual steps are buried within these terms and are not resolvable. We addressed the limitations of steady-state kinetics by developing an assay for measuring transient kinetics of CCA addition, treating the enzyme as a stoichiometric reactant relative to the substrate to allow for the isolation of specific rate and equilibrium constants. Because both the enzyme and substrate were examined at μM concentrations, similar to those in cell physiology, the information obtained by transient kinetics is biologically relevant.

Results

Kinetics of Minihelices

Extensive steady-state kinetics of minihelices has been performed with the class II *Ec*CCA. These studies support the minihelix recognition model, showing that the dihydrouridine and ASL regions are dispensable, and that the only ribose requirement for nucleotide addition is the last one in the minihelix domain.[15] For example, a 34-mer DNA minihelix based on the sequence of *E. coli* $tRNA^{Val}$ that terminates with C75 is an efficient substrate for A76 addition, exhibiting k_{cat} of 1.3 min^{-1} similar to the k_{cat} of 1.1 min^{-1} of a reconstituted full-length tRNA.[16] This DNA minihelix, designated as Val34dCr (Fig.S1), was chemically synthesized with a deoxyribose backbone up to the 1-72 base pair and a ribose backbone at positions 73-75. Similarly, DNA minihelices Val33dCr and Val32dAr that terminate with C74 and A73, respectively, are functional substrates for C75 and C74 addition [15], although in these cases oligoC synthesis is observed when CTP is present (without ATP) as the only nucleotide triphosphate.[16; 17; 18]

To extend steady-state studies of *Ec*CCA, single turnover kinetics was developed with minihelix substrates. The reaction of A76 addition to the DNA minihelix Val34dCr was performed on a rapid chemical quench instrument and was monitored by following conversion of the 5′-^{32}P-labeled minihelix to the Val35dAr product. *Ec*CCA was maintained in molar excess of the substrate to ensure only one turnover, while ATP was present at a saturating concentration (1 mM) relative to its K_m (3 μM).[17] Further increase in the ATP concentration did not increase the reaction rate. The labeled substrate and product minihelices were separated by denaturing polyacrylamide gel electrophoresis and quantified by image analysis (Fig.1B). The product conversion was nearly 100% and the time course of the conversion was well fit to a single exponential equation that describes the nature of the transient kinetics, permitting determination of the apparent rate constant k_{app} (Fig.1C). A set of controls was performed to vary systematically the reaction pH, and concentrations of Mg^{+2} and NaCl, to establish the condition that yielded the highest rate. It was also determined that quenching the reaction by

7 M urea (resulting in 5.6 M final concentration), as used in our experiments, is as effective in quenching as 500 mM EDTA.

In single turnover kinetics with enzyme in excess of the RNA substrate, the rate of nucleotide addition was found to depend on concentration of the enzyme, but not the RNA substrate. For example, pre-incubation of *Ec*CCA with Val34dCr, followed by rapid mixing with ATP, yielded time courses that increased in k_{app} with increasing concentrations of the enzyme (Fig. 1D). In contrast, fitting the time course of the reaction to a single exponential equation (% *product* = $A\times(1 - e^{-k_{app}\times t})$) over a range of different Val34dCr substrate concentrations (0.01-20 μM) in the presence of excess of enzyme did not change the first-order rate constant k_{app} (Fig.S2), while the initial rate ($V = k_{app}$ [ES]) of the reaction increased with increasing substrate concentrations. However, despite the dependence of k_{app} on *EcCCA* concentration, k_{app} increased linearly as a function of enzyme concentration up to as high as 200 μM (Fig. 1E). The linear k_{app}*vs.* concentration plot suggests that the rate of formation of the productive enzyme-substrate complex was unfavorable, and that the conditions were far away from saturation even at the highest attainable enzyme concentration. Thus, the likely interpretation of the linear plot of k_{app}*vs.* concentration is that the reaction rate is dependent on the rate of enzyme-substrate association. Under these circumstances, the slope of the plot gives an approximation of the enzyme-substrate association rate (k_{on}). This k_{on} was determined to be 7×10^3 $s^{-1}M^{-1}$ (Fig.1E), which was indeed significantly slower than the diffusion-controlled limit of 10^7-10^8 $s^{-1}M^{-1}$. The y intercept gives the k_{off} of the enzyme-substrate complex, which was determined to be 0.1 s^{-1}. The overall K_d of the enzyme-substrate complex was calculated from k_{off}/k_{on}, which yielded 14 μM, indicating a poor affinity. The slow k_{on} of the enzyme-minihelix association did not improve upon conversion of the DNA backbone of Val34dCr to the RNA backbone of Val34rCr (Fig.S3). Also, alteration of the order of premixing reactants did not improve the kinetics. For example, pre-incubation of *EcCCA* with ATP, followed by rapid mixing with Val34dCr, yielded a linear k_{app}*vs.* concentration plot with an estimated k_{on} of 11×10^3 $s^{-1}M^{-1}$, k_{off} of 0.2 s^{-1}, and K_d of 18 μM (Fig.S4A). Similarly, pre-incubation of Val34dCr with ATP, followed by rapid mixing with the enzyme, also yielded a linear k_{app}*vs.* concentration plot with an estimated k_{on} of 9×10^3 $s^{-1}M^{-1}$ (Fig.S4B). Here, the k_{off} cannot be determined with precision to calculate K_d.

Kinetics of full-length tRNAs

The above results show that, although the minihelix domain was competent for steady-state kinetics, it is inadequate for fast kinetics. To eliminate the possibility that the observed deficiency with minihelix substrates was due to defects caused by the applied reaction conditions, the full-length $tRNA_{C75}$ substrate was tested using the same reaction conditions. The full-length $tRNA_{C75}$ substrate was synthesized and labeled by run-off transcription (Fig. 2A). Formation of the enzyme-$tRNA_{C75}$ complex, followed by rapid mixing with ATP, yielded time courses that were well fit to a single-exponential equation (Fig.2B). Because the time courses showed no lags or delays, and because the plot of k_{app}*vs. Ec*CCA concentration showed saturation (Fig.2C), this suggested rapid equilibrium binding between *Ec*CCA, ATP, and the tRNA substrate, which is in contrast with the kinetics of minihelices. Fitting the plot of k_{app}*vs Ec*CCA concentration to a hyperbolic equation revealed the saturating k_{app} at 160 ± 10 s^{-1}, which is defined as the rate constant k_{A76} for A76 addition. This k_{A76} is a composite term that includes all of the events up to and including nucleotidyl transfer. The curve fitting also revealed the kinetic K_d of 0.8 ± 0.2 μM for the affinity of *Ec*CCA with $tRNA_{C75}$ (Fig.2C). Here the kinetic K_d is the K_m of the single turnover reaction (K_m(sto)). In rapid equilibrium condition, the thermodynamics of binding controls the proportion of the tRNA substrate actually bound to the enzyme and thus the reaction rate k_{app}. The kinetic K_d (or K_m(sto)) includes the possibility that a rearrangement of the initial enzyme-NTP-tRNA complex may occur to form the productive enzyme-substrate interaction. Similar results were obtained by

altering the premixing conditions. For example, premixing *Ec*CCA with ATP, followed by rapid mixing with $tRNA_{C75}$, showed saturation kinetics with k_{A76} = 170 ± 10 s^{-1} and kinetic K_d = 1.1 ± 0.3 μM (Fig.S5A). Premixing $tRNA_{C75}$ with ATP, followed by rapid mixing with *Ec*CCA, showed saturation kinetics with k_{A76} = 130 ± 10 s^{-1} and kinetic K_d = 2.4 ± 0.2 μM (Fig.S5B).

The contrast between the full-length $tRNA_{75C}$ and minihelices in fast kinetics emphasized that the tRNA whole body is necessary for high affinity and rapid productive binding to the enzyme. Moreover, the k_{A76} value in the range of 130-170 s^{-1} for $tRNA_{C75}$ is comparable to the k_{pol} value of 220 s^{-1} of the template-dependent T7 RNA polymerase,[19] indicating that the rate-determining steps of these enzymes take place in similar time scales. The kinetic K_d of 0.8-2.4 μM for the enzyme affinity to $tRNA_{C75}$ is in the range of the physiological concentration of tRNA precursors, estimated at ~2 μM.[3]

Characterization of nicked tRNAs

An earlier study showed that *Ec*CCA has a phosphohydrolase activity that repairs aberrant tRNA 3′ ends before nucleotide addition.[20] The ability of *Ec*CCA to discriminate against minihelices suggested the further possibility that the enzyme might inspect the tRNA whole body to reject nicks in the tRNA phosphodiester backbone. To test this possibility, two nicked substrates were prepared (Fig.S1). One was formed by hybridization of the G1-G57 fragment of *E. coli* $tRNA^{Val}$ with the chemically synthesized A58-C75 fragment to produce a nick in the T loop of the minihelix domain. Such a T-nicked substrate has been shown to be functional for recognition by *Ec*CCA in steady-state kinetics.[16] Also, a similar approach was used earlier to create a T-nicked substrate in the sequence framework of *E. coli* $tRNA^{Pro}$, which was shown to be functional for aminoacylation by *E. coli* prolyl-tRNA synthetase,[21] an enzyme that recognizes the tRNA global structure.[22] The other nicked substrate of *E. coli* $tRNA^{Val}$ was formed by hybridization of the G1-A37 fragment of the tRNA with the G38-C75 fragment to produce a nick in the ASL. In this case, the G38-C75 fragment replaced the natural A38 with G38 to allow efficient transcription *in vitro*. A similar ASL-nicked tRNA in the sequence framework of *E. coli* $tRNA^{Gln}$ has been previously constructed, where the backbone nick was readily sealed by T4 RNA ligase to generate an intact tRNA that is recognized by *E. coli* glutaminyl-tRNA synthetase,[23] which also recognizes the tRNA global structure for aminoacylation.

In preparation of the two nicked substrates of *E. coli* $tRNA^{Val}$, the 3′ fragment was labeled with ^{32}P to allow analysis of hybridization by gel electrophoresis in native conditions containing 10 mM $MgCl_2$. Hybridization analysis revealed two products in the generation of the T-nicked substrate (Fig.3A, left), and one major and one minor product in the generation of the ASL-nicked substrate (Fig.3A, right). In both cases, the major product (indicated by red arrows) exhibited the same gel mobility as that of the intact and full-length tRNA and was isolated from the native gel and used as the nicked substrate, whereas the minor product (indicated by black arrows) exhibited aberrant gel mobility and was not used. Both the gel purified T- and ASL-nicked substrates were determined for their concentrations by UV absorption.

Because the ASL-nicked substrate has the A38G substitution (Fig.3B), which can induce an aberrant folding (Fig.3C), this nicked substrate was characterized further. The following three experiments support the notion that the ASL-nicked substrate, as isolated from Fig.3A, existed in the proposed canonical structure (Fig.3B). First, the ASL-nicked substrate is readily ligated by T4 RNA ligase 2 (ref24) to 55% (data not shown). This high efficiency of ligation is not expected for the putative aberrant structure, which is unfavorable for ligation. Second, the ASL-nicked substrate is aminoacylated by *E. coli* ValRS with better efficiency than the minor species, which might represent the aberrant ASL-nicked tRNA (designated as such in Fig.3D).

The rationale of this experiment was based on extensive structural and biochemical studies of the $tRNA^{Val}$-ValRS interaction, which must depend on direct enzyme recognition of the tRNA anticodon nucleotides.[25] In the canonical structure, the anticodon nucleotides are accessible for recognition, although the presence of the nick adjacent to the anticodon triplet is expected to reduce the aminoacylation activity relative to that of the intact tRNA. However, in the putative aberrant structure, the anticodon nucleotides are inaccessible, preventing recognition by ValRS. Importantly, aminoacylation analysis also showed that the intact A38G mutant retained the activity of the wild-type tRNA, indicating that the A38G substitution did not significantly alter the tRNA structure. Third, the ASL-nicked substrate was competent for lead cleavage (Fig.3E). The metal ion lead induces cleavage between nucleotide 17 and the conserved G18 in the canonical tRNA tertiary core.[26] This cleavage is coordinated by precise positioning of lead in a pocket formed by conserved residues in the D and T loops.[27] Substitutions in the tRNA tertiary core can eliminate lead cleavage.[27] Notably, the intact A38G mutant of $tRNA^{Val}$ was a functional substrate for lead cleavage, generating a large fragment of 59-mer and a smaller fragment of 17-mer. These fragments were well resolved by a 12% denaturing PAGE (Fig.3E). The ASL-nicked A38G mutant dissociated in the denaturing PAGE into a mixture of two co-migrating fragments, a 39-mer and a 37-mer. Upon incubation of the ASL-nicked substrate with lead ions under native conditions, one of the co-migrating fragments (the 37-mer) was cleaved into 17- and 20-mer fragments, while the 39-mer fragment remained intact. This cleavage pattern is consistent with the presence of a prominent Pb^{+2} cleavage site in the D/T loop region, suggesting that the ASL-nicked tRNA basically adopts the canonical L-shaped tRNA fold. Together, the above results support the notion that the ASL-nicked tRNA adopts the normal tRNA structure that is recognized for ligation, for aminoacylation, and for lead cleavage.

Kinetics of nicked tRNAs

Single turnover kinetics of A76 addition to both the T-nicked and ASL-nicked substrates was measured by mixing a preformed *Ec*CCA-substrate complex with ATP. Both nicked substrates were competent for CCA addition, with more than 90% of substrate converted to product at the end of the reaction. However, the T-nicked substrate exhibited slow kinetics, with k_{app}s ~1000-fold lower than those of the intact $tRNA_{C75}$ at equivalent enzyme concentrations (Fig. 4A). A plot of k_{app}*vs.* enzyme concentration was linear up to 100 μM *Ec*CCA with a slow k_{on} of 7×10^3 $s^{-1}M^{-1}$ (Fig.4A, inset) in a pattern similar to that of minihelices. The ASL-nicked substrate also exhibited a slower rate, but the kinetics of k_{app}*vs.* enzyme concentration showed saturation, permitting the determination of k_{A76} (170 ± 10 s^{-1}), similar to that of the intact tRNA, but a 10-fold higher kinetic K_d (8.6 ± 1.3 μM) for enzyme-substrate association (Fig. 4A). Thus, *Ec*CCA discriminates against the ASL nick by reducing the affinity to the nicked substrate. Once stably bound to the nicked substrate, the enzyme catalyzes A76 addition at a rate identical to that of the intact tRNA.

The kinetic discrimination of *Ec*CCA against minihelices and nicked tRNA substrates was further demonstrated for C75 and C74 addition. C75 addition to the minihelix Val33dCr, performed in the presence of a saturating concentration of CTP (5 mM), produced oligoC (Fig.S6A,B), consistent with previous observations.[17; 18] In this case, the rate of C75 addition based on summing all the products of oligoC synthesis was the same as the rate based on substrate consumption. However, measurement of k_{app} as a function of *Ec*CCA concentration showed a linear increase of the rate with a rather slow k_{on} of 250 $s^{-1}M^{-1}$ (Fig.S6C,D). In contrast, C75 addition to the full-length $tRNA_{C74}$ manifested two major improvements. First, the addition was precisely one nucleotide without synthesis of oligoC (Fig.S7A,B), indicating that the presence of the tRNA whole body strengthened the specificity of the enzyme. Second, the kinetics of C75 addition was saturable (Fig.S7C,D) with k_{C75} = 170 ± 20 s^{-1} and kinetic K_d = 2.8 ± 0.8 μM of the $tRNA_{C74}$ substrate. Furthermore, introduction of a backbone nick

between positions 37-38 in the ASL increased the kinetic K_d to 17.5 ± 3.8 μM but had little effect on k_{C75} (180 ± 20 s^{-1}) (Fig.4B), indicating discrimination at the binding step. These observations were recapitulated for C74 addition. In the presence of CTP only, the Val32dAr minihelix was a substrate for both C74 addition and oligoC synthesis (Fig.S8A,B), and the kinetics of nucleotide addition revealed a linear increase of k_{app} as a function of enzyme concentration, exhibiting an even slower k_{on} of 25 $s^{-1}M^{-1}$ (Fig.S8C,D) than that for C75 addition. In contrast, the full-length $tRNA_{A73}$ was an efficient substrate for C74 addition, which was rapidly followed by C75 addition (Fig.S9A,B). Kinetic analysis revealed a saturating k_{C74} of 170 ± 20 s^{-1} and a kinetic K_d of 3.3 ± 0.8 μM for the $tRNA_{A73}$ substrate (Fig.S9C,D). Also, introduction of a backbone nick at positions 37-38 raised the kinetic K_d to 16.9 ± 4.2 μM, but had only a small effect on k_{C74} (150 ± 10 s^{-1}) (Fig.4C).

Discussion

The kinetic parameters of A76, C75, and C74 addition to the full-length and ASL-nicked $tRNA^{Val}$ substrates by *Ec*CCA are summarized in Table 1. With the full-length tRNA, the enzyme catalyzes rapid nucleotide addition with a similar rate at all three steps and has a physiologically relevant high affinity. However, introduction of a backbone break to the ASL, the domain that is separate from the CCA end by the longest distance (~75 Å) in tRNA, reduces the enzyme affinity to the nicked-substrate, suggesting that the proper activity of the minihelix domain for CCA addition is dependent on the integrity of the ASL. The overall discrimination against the nick for each nucleotide addition is manifested by the ratio of the specificity factor k_N/K_d for the intact tRNA over the factor for the nicked substrate. This discrimination increases from 5.7-fold for C74 addition, to 6.1-fold for C75 addition, to 10.6-fold for A76 addition, indicating a progressively closer scrutiny of the tRNA substrate as the enzyme approaches completion of CCA synthesis. The discrimination against the T-nicked substrate is even stronger, because reactions did not reach saturation even at high enzyme concentrations (~100 μM). This is rationalized by the fact that the nick is localized in the miniehelix domain, which is in direct contact with the enzyme.

The discrimination against backbone nicks by *Ec*CCA is likely shared in common by all class II CCA enzymes (including those of eukaryotes), given the similar properties of substrate recognition among members of this class.[29] In the lifetime of tRNA biosynthesis, backbone nicks can be generated in a number of ways. For example, misincorporation of nucleotides, inappropriate processing and folding, or incomplete post-transcriptional modifications in tRNA[30] can lead to aberrant tertiary structures that are prone to nuclease cleavage. Some bacterial and eukaryotic tRNAs are also subject to cleavage at the ASL by specific toxins.[31; 32] In eukaryotes, the ASL is the site that carries introns for certain tRNA precursors (usually between positions 37-38 as designated in Fig.S1). Splicing intermediates without properly religated backbones that accumulate in cells have been identified.[33] Discrimination of these nicked tRNAs from CCA addition offers a quality control mechanism that is manifested at the kinetic level. Based on the estimated cellular concentration of CCA enzyme at ~0.8 μM [calculated from ref[3]], the kinetic quality control ensures that only full-length and intact tRNAs are subject to rapid CCA addition at a rate of ~30, 40, and 80 s^{-1} for addition of C74, C75, and A76, respectively (e.g., $k_{app} = \frac{k_{76} \times [Enz]}{K_d + [Enz]}$). As such, tRNAs with the CCA sequence can quickly continue on in the maturation process or proceed to reactions for protein synthesis, which in turn provide protein-binding partners (such as aminoacyl-tRNA synthetases, elongation factors, and the ribosome) that protect the CCA sequence. In contrast, the backbone-nicked tRNAs are rejected by the CCA enzyme and, without protein protection, are rapidly degraded by the various tRNA surveillance machineries that have been discovered in both *E. coli* and yeast.[30; 34; 35]

The synthesis and maintenance of the CCA sequence confers "eligibility" to a tRNA for participation in protein synthesis, even if the tRNA is still at an early stage in the maturation process (such as in the nucleus). Protein synthesis is a multi-step process that requires energy consumption for aminoacylation of a matured tRNA, for accommodation of the aminoacylated tRNA at the ribosome, and for translocation of the tRNA through the ribosome after peptide bond formation. Thus, in the overall maturation process of a tRNA, CCA addition represents an important checkpoint prior to becoming eligible for protein synthesis. The quality control of CCA addition at the checkpoint can ensure that only backbone-intact tRNAs remain in the active processing pathway as substrates for both the repair and *de novo* biosynthesis functions of the CCA enzyme. For example, in *E. coli*, where the CCA sequence is encoded in all tRNA genes, *Ec*CCA functions to regenerate missing nucleotides from the CCA sequence that are removed by nucleases. In bacteria (such as *Bacillus subtilis*) that do not encode the CCA sequence in some of their tRNA genes, precursor tRNAs must be processed by endonucleases to remove 3′ trailer sequences,[36] and the CCA sequence added *de novo* as a prerequisite for efficient processing of the 5′ end.[37; 38] A similar situation exists in the eukaryotic nucleus, where the CCA sequence is a determinant for nuclear tRNA aminoacylation and for export of tRNA with correctly processed 5′ and 3′ ends.[39; 40; 41]

This study demonstrates that, although tRNA minihelices are competent in steady-state kinetics and appear to embody all of the binding interactions with both classes of CCA enzymes, they are not sufficient for fast CCA addition. The minihelix domain is thought to have evolved earlier than the anticodon domain to serve as a tag for the replication of primitive RNA genomes.[42; 43] Indeed, minihelices that carry major determinants for various tRNA functions have been reported. For example, the minihelix domain is recognized by RNase P for processing 5′ leader sequences[44], and it provides the primary contact site for recognition of aminoacyl-tRNA by bacterial elongation factor EF-Tu.[45; 46] The minihelix of $tRNA^{Ala}$ serves as the aminoacylation domain of the bacterial tmRNA molecule that tags proteins synthesized from damaged mRNAs to degradation.[47] Importantly, the minihelix domain of $tRNA^{Ala}$ contains the G3:U70 major determinant for aminoacylation with alanine.[48; 49] Although the domain by itself retains the specificity of aminoacylation, its catalytic efficiency (k_{cat}/K_m) is reduced from that of the full-length tRNA.[50] Upon analysis by single turnover kinetics, the minihelix domain is likely to be further reduced relative to that of the full-length tRNA. The inefficient interaction of the isolated minihelix domain with *Ec*CCA, and perhaps with other enzymes as well, may arise from the fact that, although the isolated minihelix domain recapitulates the sequence of the coaxially stacked acceptor stem and T stem-loop, it lacks the support from interactions with the D loop. This could affect the conformation of the T loop and/or reduce the conformational rigidity of the acceptor-T stem module. Also, as seen in the crystal structure of yeast $tRNA^{Phe}$ (ref 9), the coaxial stacking of the acceptor stem and T stem-loop has a small angle of 14° (ref 28), which may not be properly maintained in the absence of the D and T loop interactions.

Our results here demonstrate that tRNA domains distal from the minihelix domain (such as ASL) are determinants for rapid activity of CCA addition. Similarly, a recent study demonstrates that, although the ASL of a tRNA provides all the information necessary for the anticodon-codon base pairing interaction on the ribosome, the region of the tRNA distal from the ASL, which involves the D stem of the tRNA tertiary core, influences the fidelity of the anticodon-codon base pairing.[51] These studies, together with those mentioned above of minihelices, emphasize the notion that individual tRNA domains exhibit their biologically relevant functions only in the context of the entire tRNA molecule, even though these domains in isolation appear to possess the sequence and structural information required for function. This notion is likely to hold in the interaction of tRNA with other protein-binding partners, such as those required for tRNA modification and processing. In the context of the tRNA whole body, we further show that *Ec*CCA effectively discriminates against backbone nicks or damage

at each step of CCA addition, offering a previously unrecognized surveillance step before committing tRNA molecules to protein synthesis.

Materials and Methods

Preparation of *EcCCA*

A previous over-expression clone of wild-type *E. coli cca* gene was constructed by inserting the gene between the *Nde*I and *Bam*H1 sites of pET-22b(+) (Novagen) and by changing the TGA stop codon to the CTA leucine codon.[18] Site-directed mutagenesis by QuikChange (Stratagene) was performed on this clone to remove most of the C-terminal extension sequence, leaving only a glycine codon between the leucine codon of the gene and the His-tag. The modified plasmid was transformed into *E. coli* BL21(DE3) and enzyme expression was induced for 4 h with 0.3 mM IPTG at 37°C. The collected cells were sonicated and lysed in 20 mM Tris-HCl pH 8.0, 500 mM NaCl, 6 mM $MgCl_2$, 5 mM imidazole, 3 mM β-mercaptoethanol, 5% glycerol). *Ec*CCA was bound to the Co^{2+}-chelated TALON resin (ClonTech) and eluted with 25-50 mM of imidazole. The fractions with the highest contents of *Ec*CCA were pooled, concentrated, and exchanged into storage buffer of 100 mM glycine pH 9.0, 50 mM NaCl, 2 mM $MgCl_2$, 1 mM β-mercaptoethanol, and 40% glycerol. Enzyme concentration was determined by Bradford assay.

Substrate preparation

DNA minihelices Val34dCr, Val33dCr, and Val32dAr, containing ribose moieties starting at position 73, and RNA minihelix Val34rCr were chemically synthesized by IDT (Coralville) and used directly. The full-length substrates of *E. coli* $tRNA^{Val}$, $tRNA_{C75}$, $tRNA_{C74}$, and $tRNA_{A73}$ were prepared by run-off transcription by T7 RNA polymerase based on template sequences synthesized from overlapping oligonucleotides. The full-length transcripts were separated from their templates and unincorporated NTPs by 12% denaturing PAGE/7M urea, localized by UV shadowing, and extracted from gels. The T-nicked substrate was prepared by annealing the G1-G57 fragment (transcribed by T7 RNA polymerase) with the A58-C75 RNA fragment (synthesized by IDT). The ASL-nicked substrate was prepared by annealing the G1-A37 fragment (transcribed by T7 RNA polymerase) with the G38-C75 RNA fragment (which contained the A38G substitution and was transcribed by T7 RNA polymerase). Both nicked substrates was formed by heating a mixture of the 5′ fragment in 2-fold molar excess of the 3′ fragment at 90°C for 3 minutes, followed by slow cooling to 37°C for 10 minutes. The annealed mixtures were separated by a non-denaturing 12% PAGE/90 mM Tris pH 8.0, 90 mM borate and 10 mM $MgCl_2$ (TBM) gel, and the annealed hybrids that co-migrated with a full-length tRNA standard were extracted from gels and eluted in 10 mM Tris, pH 8.0. The nicked tRNA substrates were precipitated by ethanol and stored in 10 mM Tris-HCl, pH 8.0 and 1 mM $MgCl_2$. Such nicked substrates migrated to the same electrophoretic position as the intact full-length tRNA on native gel analysis, indicating that the fragments in the nicked substrate did not dissociate during gel elution. Concentrations of full-length and nicked substrates were determined by UV absorption.

Minihelices and the 3′ fragment of the T-nicked substrate were labeled at the 5′ end with γ-^{32}P-ATP (3000 Ci/mmol, Perkin Elmer) by T4 polynucleotide kinase (NEB) for 45 minutes at 37°C. After heat inactivation of the kinase, the labeled substrates were separated from free ATP by a Centrispin-20 column (Princeton Separation). The full-length tRNAs and 3′ fragments of the ASL-nicked substrates were labeled internally by using α-^{32}P-ATP (3000 Ci/mmol, Perkin Elmer) during the T7 transcription and were purified by 12% PAGE/7M urea.

Single turnover kinetics

Single turnover assays were performed using an RQF-3 (KinTek). The reaction buffer for minihelices contained 1 mM DTT, 50 or 100 mM glycine (pH 9.0), 5 or 10 mM $MgCl_2$ and 10% glycerol (including glycerol contributed by the enzyme storage buffer), and the saturating concentration of a specific nucleoside triphosphate (1 mM ATP or 5 mM CTP). Increasing concentrations of *Ec*CCA, as annotated in the figures, were mixed with 50 nM of a minihelix substrate. For the full-length tRNA substrate, both the enzyme and substrate concentrations increased but maintained at a fixed 10:1 molar ratio. For each reaction, 10 μl of each syringe was loaded into the instrument. After different reaction times (0.1 to 300 s for the minihelices and the T-nicked tRNA, 2 to 70 ms for the tRNAs), the reactions were quenched with 80 μl of 7 M urea quench solution. The reaction samples were separated on a 12% PAGE/7M urea gel, exposed to a phosphor screen, scanned with Storm 820 and analyzed with ImageQuant 5.2 software (GE Healthcare).

The fraction of product formation was calculated based on the % of substrate that was converted to product. The fraction of substrate conversion over time was fit to a single exponential equation: $\%product = A\times(1\text{-}e^{-k_{app}\times t})$, where A is the amplitude, t is the time and k_{app} is the observed rate constant of the A76, C75, or C74 incorporation, respectively. The data of k_{app}*vs.* enzyme concentration were fit to a hyperbolic equation: $k_{app} = \frac{k_{76}\times[\mathrm{Enz}]}{K_d + [\mathrm{Enz}]}$, where k_{76} is the catalytic rate constant and K_d is the dissociation constant. Alternatively, a linear fit was obtained: $k_{app} = k_{off} + k_{on}\times[Enz]$, where k_{off} is the intercept and k_{on} is the association rate constant.

Aminoacylation and lead cleavage analysis

Aminoacylation of $tRNA^{Val}$ transcripts (2 μM) by purified *E. coli* ValRS (4 μM) at 37 °C in 50 mM Tris-HCl, pH 7.5, 20 mM KCl, 4.0 mM DTT, 0.2 mg/mL BSA, 10 mM $MgCl_2$, 2.0 mM ATP, and 20 μM [^{3}H]-valine (15,600 dpm/pmole). The activity of aminoacylation was measured by monitoring the enzyme-catalyzed synthesis of [^{3}H]-val-$tRNA^{Val}$ collected on filter pads in 5% TCA (trichloroacetic acid). Lead cleavage was performed by incubating lead acetate (1 mM) with intact or ASL-nicked A38G mutant of *E. coli* $tRNA^{Val}$ (1.0 and 2.5 μg, respectively) in 25 mM MOPS, pH 7.0, 1.5 mM spermine, 15 mM $MgCl_2$ for 20 min at 42 ° C. The reaction was terminated by the denaturing loading dye and the cleavage products were resolved by 12% denaturing PAGE.

Supplementary Material

Refer to Web version on PubMed Central for supplementary material.

Acknowledgements

We thank Catherine Joyce for advice, Alan Weiner for encouragement, and Eric Phizicky, Murray Deutscher, Ken Johnson, and Jon Lorsch for comments on the manuscript. We also thank the anonymous reviewers for very helpful suggestions. This work was supported by NIH grant GM068561 to YMH.

References

1. Deutscher MP. tRNA nucleotidyltransferase. Enzymes 1982;15:183–215.
2. Aebi M, Kirchner G, Chen JY, Vijayraghavan U, Jacobson A, Martin NC, Abelson J. Isolation of a temperature-sensitive mutant with an altered tRNA nucleotidyltransferase and cloning of the gene encoding tRNA nucleotidyltransferase in the yeast Saccharomyces cerevisiae. J Biol Chem 1990;265:16216–20. [PubMed: 2204621]

3. Yue D, Maizels N, Weiner AM. CCA-adding enzymes and poly(A) polymerases are all members of the same nucleotidyltransferase superfamily: characterization of the CCA-adding enzyme from the archaeal hyperthermophile Sulfolobus shibatae. Rna 1996;2:895–908. [PubMed: 8809016]
4. Yue D, Weiner AM, Maizels N. The CCA-adding enzyme has a single active site. J Biol Chem 1998;273:29693–700. [PubMed: 9792681]
5. Li F, Xiong Y, Wang J, Cho HD, Tomita K, Weiner AM, Steitz TA. Crystal structures of the Bacillus stearothermophilus CCA-adding enzyme and its complexes with ATP or CTP. Cell 2002;111:815–24. [PubMed: 12526808]
6. Xiong Y, Li F, Wang J, Weiner AM, Steitz TA. Crystal structures of an archaeal class I CCA-adding enzyme and its nucleotide complexes. Mol Cell 2003;12:1165–72. [PubMed: 14636575]
7. Okabe M, Tomita K, Ishitani R, Ishii R, Takeuchi N, Arisaka F, Nureki O, Yokoyama S. Divergent evolutions of trinucleotide polymerization revealed by an archaeal CCA-adding enzyme structure. Embo J 2003;22:5918–27. [PubMed: 14592988]
8. Augustin MA, Reichert AS, Betat H, Huber R, Morl M, Steegborn C. Crystal Structure of the Human CCA-adding Enzyme: Insights into Template-independent Polymerization. J Mol Biol 2003;328:985–94. [PubMed: 12729736]
9. Xiong Y, Steitz TA. Mechanism of transfer RNA maturation by CCA-adding enzyme without using an oligonucleotide template. Nature 2004;430:640–5. [PubMed: 15295590]
10. Tomita K, Fukai S, Ishitani R, Ueda T, Takeuchi N, Vassylyev DG, Nureki O. Structural basis for template-independent RNA polymerization. Nature 2004;430:700–4. [PubMed: 15295603]
11. Tomita K, Ishitani R, Fukai S, Nureki O. Complete crystallographic analysis of the dynamics of CCA sequence addition. Nature 2006;443:956–60. [PubMed: 17051158]
12. Shi PY, Maizels N, Weiner AM. CCA addition by tRNA nucleotidyltransferase: polymerization without translocation? Embo J 1998;17:3197–206. [PubMed: 9606201]
13. Cho HD, Chen Y, Varani G, Weiner AM. A model for C74 addition by CCA-adding enzymes: C74 addition, like C75 and A76 addition, does not involve tRNA translocation. J Biol Chem 2006;281:9801–11. [PubMed: 16455665]
14. Cho HD, Verlinde CL, Weiner AM. Archaeal CCA-adding enzymes: central role of a highly conserved beta-turn motif in RNA polymerization without translocation. J Biol Chem 2005;280:9555–66. [PubMed: 15590678]
15. Shi PY, Weiner AM, Maizels N. A top-half tDNA minihelix is a good substrate for the eubacterial CCA- adding enzyme. Rna 1998;4:276–84. [PubMed: 9510330]
16. Seth M, Thurlow DL, Hou YM. Poly(C) synthesis by class I and class II CCA-adding enzymes. Biochemistry 2002;41:4521–32. [PubMed: 11926813]
17. Hou YM, Gu SQ, Zhou H, Ingerman L. Metal-Ion-Dependent Catalysis and Specificity of CCA-Adding Enzymes: A Comparison of Two Classes. Biochemistry 2005;44:12849–59. [PubMed: 16171400]
18. Hou YM. Unusual synthesis by the Escherichia coli CCA-adding enzyme [In Process Citation]. Rna 2000;6:1031–43. [PubMed: 10917598]
19. Anand VS, Patel SS. Transient state kinetics of transcription elongation by T7 RNA polymerase. J Biol Chem 2006;281:35677–85. [PubMed: 17005565]
20. Yakunin AF, Proudfoot M, Kuznetsova E, Savchenko A, Brown G, Arrowsmith CH, Edwards AM. The HD domain of the Escherichia coli tRNA nucleotidyltransferase has 2′,3′-cyclic phosphodiesterase, 2′-nucleotidase, and phosphatase activities. J Biol Chem 2004;279:36819–27. [PubMed: 15210699]
21. Yap LP, Stehlin C, Musier-Forsyth K. Use of semi-synthetic transfer RNAs to probe molecular recognition by Escherichia coli proline-tRNA synthetase. Chem Biol 1995;2:661–6. [PubMed: 9383472]
22. Liu H, Peterson R, Kessler J, Musier-Forsyth K. Molecular recognition of tRNA(Pro) by Escherichia coli proline tRNA synthetase in vitro. Nucleic Acids Res 1995;23:165–9. [PubMed: 7870582]
23. Sherlin LD, Bullock TL, Nissan TA, Perona JJ, Lariviere FJ, Uhlenbeck OC, Scaringe SA. Chemical and enzymatic synthesis of tRNAs for high-throughput crystallization. Rna 2001;7:1671–8. [PubMed: 11720294]

24. Nandakumar J, Shuman S. Dual mechanisms whereby a broken RNA end assists the catalysis of its repair by T4 RNA ligase 2. J Biol Chem 2005;280:23484–9. [PubMed: 15851476]
25. Fukai S, Nureki O, Sekine S, Shimada A, Tao J, Vassylyev DG, Yokoyama S. Structural basis for double-sieve discrimination of L-valine from L- isoleucine and L-threonine by the complex of tRNA (Val) and valyl-tRNA synthetase. Cell 2000;103:793–803. [PubMed: 11114335]
26. Krzyzosiak WJ, Marciniec T, Wiewiorowski M, Romby P, Ebel JP, Giege R. Characterization of the lead(II)-induced cleavages in tRNAs in solution and effect of the Y-base removal in yeast tRNAPhe. Biochemistry 1988;27:5771–7. [PubMed: 3179275]
27. Behlen LS, Sampson JR, DiRenzo AB, Uhlenbeck OC. Lead-catalyzed cleavage of yeast tRNAPhe mutants. Biochemistry 1990;29:2515–23. [PubMed: 2334679]
28. Holbrook SR, Sussman JL, Warrant RW, Kim SH. Crystal structure of yeast phenylalanine transfer RNA. II. Structural features and functional implications. J Mol Biol 1978;123:631–60. [PubMed: 357743]
29. Cho HD, Oyelere AK, Strobel SA, Weiner AM. Use of nucleotide analogs by class I and class II CCA-adding enzymes (tRNA nucleotidyltransferase): deciphering the basis for nucleotide selection. Rna 2003;9:970–81. [PubMed: 12869708]
30. Alexandrov A, Chernyakov I, Gu W, Hiley SL, Hughes TR, Grayhack EJ, Phizicky EM. Rapid tRNA decay can result from lack of nonessential modifications. Mol Cell 2006;21:87–96. [PubMed: 16387656]
31. Ogawa T, Tomita K, Ueda T, Watanabe K, Uozumi T, Masaki H. A cytotoxic ribonuclease targeting specific transfer RNA anticodons. Science 1999;283:2097–100. [PubMed: 10092236]
32. Lu J, Huang B, Esberg A, Johansson MJ, Bystrom AS. The Kluyveromyces lactis gamma-toxin targets tRNA anticodons. Rna 2005;11:1648–54. [PubMed: 16244131]
33. Ho CK, Rauhut R, Vijayraghavan U, Abelson J. Accumulation of pre-tRNA splicing '2/3' intermediates in a Saccharomyces cerevisiae mutant. Embo J 1990;9:1245–52. [PubMed: 2182322]
34. Li Z, Reimers S, Pandit S, Deutscher MP. RNA quality control: degradation of defective transfer RNA. Embo J 2002;21:1132–8. [PubMed: 11867541]
35. Kadaba S, Krueger A, Trice T, Krecic AM, Hinnebusch AG, Anderson J. Nuclear surveillance and degradation of hypomodified initiator tRNAMet in S. cerevisiae. Genes Dev 2004;18:1227–40. [PubMed: 15145828]
36. Deutscher MP. Degradation of RNA in bacteria: comparison of mRNA and stable RNA. Nucleic Acids Res 2006;34:659–66. [PubMed: 16452296]
37. Wegscheid B, Hartmann RK. The precursor tRNA 3′-CCA interaction with Escherichia coli RNase P RNA is essential for catalysis by RNase P in vivo. Rna 2006;12:2135–48. [PubMed: 17135488]
38. Wegscheid B, Hartmann RK. In vivo and in vitro investigation of bacterial type B RNase P interaction with tRNA 3′-CCA. Nucleic Acids Res 2007;35:2060–73. [PubMed: 17355991]
39. Lund E, Dahlberg JE. Proofreading and aminoacylation of tRNAs before export from the nucleus [see comments]. Science 1998;282:2082–5. [PubMed: 9851929]
40. Sarkar S, Azad AK, Hopper AK. Nuclear tRNA aminoacylation and its role in nuclear export of endogenous tRNAs in Saccharomyces cerevisiae. Proc Natl Acad Sci U S A 1999;96:14366–71. [PubMed: 10588711]
41. Grosshans H, Hurt E, Simos G. An aminoacylation-dependent nuclear tRNA export pathway in yeast. Genes Dev 2000;14:830–40. [PubMed: 10766739]
42. de Duve C. Transfer RNAs: the second genetic code. Nature 1988;333:117–8. [PubMed: 3367984]
43. Weiner AM, Maizels N. tRNA-like structures tag the 3′ ends of genomic RNA molecules for replication: implications for the origin of protein synthesis. Proc Natl Acad Sci U S A 1987;84:7383–7. [PubMed: 3478699]
44. McClain WH, Guerrier-Takada C, Altman S. Model substrates for an RNA enzyme. Science 1987;238:527–30. [PubMed: 2443980]
45. Nissen P, Kjeldgaard M, Thirup S, Polekhina G, Reshetnikova L, Clark BF, Nyborg J. Crystal structure of the ternary complex of Phe-tRNAPhe, EF-Tu, and a GTP analog [see comments]. Science 1995;270:1464–72. [PubMed: 7491491]

46. Nissen P, Thirup S, Kjeldgaard M, Nyborg J. The crystal structure of Cys-tRNACys-EF-Tu-GDPNP reveals general and specific features in the ternary complex and in tRNA. Structure 1999;7:143–56. [PubMed: 10368282]

47. Keiler KC, Waller PR, Sauer RT. Role of a peptide tagging system in degradation of proteins synthesized from damaged messenger RNA [see comments]. Science 1996;271:990–3. [PubMed: 8584937]

48. Hou YM, Schimmel P. A simple structural feature is a major determinant of the identity of a transfer RNA. Nature 1988;333:140–5. [PubMed: 3285220]

49. McClain WH, Foss K. Changing the identity of a tRNA by introducing a G-U wobble pair near the 3′ acceptor end. Science 1988;240:793–6. [PubMed: 2452483]

50. Francklyn C, Schimmel P. Aminoacylation of RNA minihelices with alanine. Nature 1989;337:478–81. [PubMed: 2915692]

51. Cochella L, Green R. An active role for tRNA in decoding beyond codon:anticodon pairing. Science 2005;308:1178–80. [PubMed: 15905403]

52. Hauenstein S, Zhang CM, Hou YM, Perona JJ. Shape-selective RNA recognition by cysteinyl-tRNA synthetase. Nat Struct Mol Biol 2004;11:1134–41. [PubMed: 15489861]

53. Kim SH, Suddath FL, Quigley GJ, McPherson A, Sussman JL, Wang AH, Seeman NC, Rich A. Three-dimensional tertiary structure of yeast phenylalanine transfer RNA. Science 1974;185:435–40. [PubMed: 4601792]

54. Robertus JD, Ladner JE, Finch JT, Rhodes D, Brown RS, Clark BF, Klug A. Structure of yeast phenylalanine tRNA at 3 A resolution. Nature 1974;250:546–51. [PubMed: 4602655]

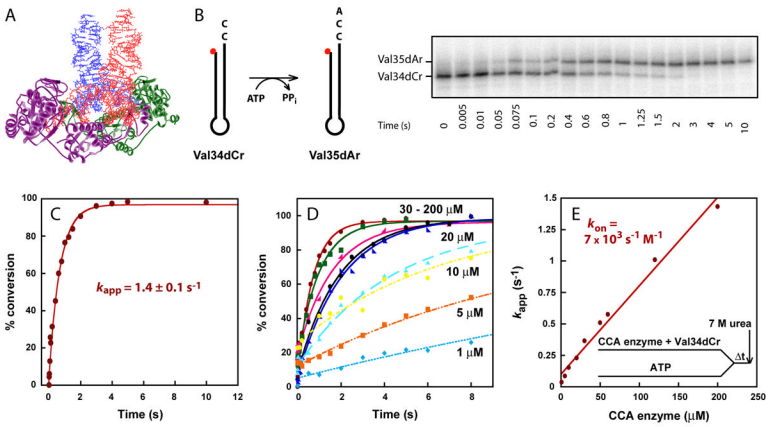

Figure 1.

(A) Crystal structure of the dimer of *Af*CCA-tRNA complex (PDB 1SZ1). The tRNA backbone is highlighted in red and blue, whereas *Af*CCA subunits are represented by purple and green ribbons. (B) A schematic drawing of the Val34dCr minihelix substrate for A76 addition, using ATP as the nucleotide donor. The minihelix is 5′-labeled with ^{32}P (50 nM), indicated by a red dot, and the time course of conversion to Val35dCr catalyzed by *Ec*CCA (200 μM) is analyzed by 12% PAGE/7M urea. The nomenclature of minihelices is established by the identity of the tRNA (Val), the length of the minihelices (from a 34- to 35-mer), the DNA backbone (d), and the terminal ribose residue (from Cr to Ar). (C) Fitting the data of the time course in (B) to a single exponential equation to derive the $k_{app} = 1.4 \pm 0.1\ s^{-1}$. (D) Representative time courses of A76 addition to Val34dCr by increasing concentration of *Ec*CCA (1-200 μM, as shown). Reactions were performed by pre-incubating *Ec*CCA with the minihelix substrate, followed by rapid mixing with ATP (1 mM) over various time periods, then terminated by mixing with 7 M urea as shown in (E). (E) The linear increase of k_{app} as a function of *Ec*CCA concentration based on data of (D), giving an estimated k_{on} of $7 \times 10^3\ s^{-1}M^{-1}$.

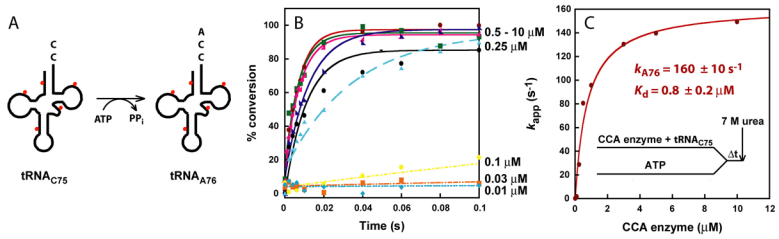

Figure 2.

(A) A schematic drawing of the $tRNA_{75C}$ substrate for A76 addition, using ATP as the nucleotide donor. The tRNA is labeled during transcription by incorporation of [α-^{32}P]AMP, indicated by red dots. (B) Representative time courses of A76 addition to $tRNA_{75C}$ by increasing concentration of *Ec*CCA (0.01-10 μM, as shown). Reactions were performed by pre-incubating *Ec*CCA with $tRNA_{75C}$ (maintained at 1/10 below the concentration of *Ec*CCA), followed by rapid mixing with ATP (1 mM) over various time periods, then terminated by mixing with 7 M urea as shown in (C). (C) Fitting the data of (B) to a hyperbolic equation to derive k_{A76} and K_d for $tRNA_{C75}$.

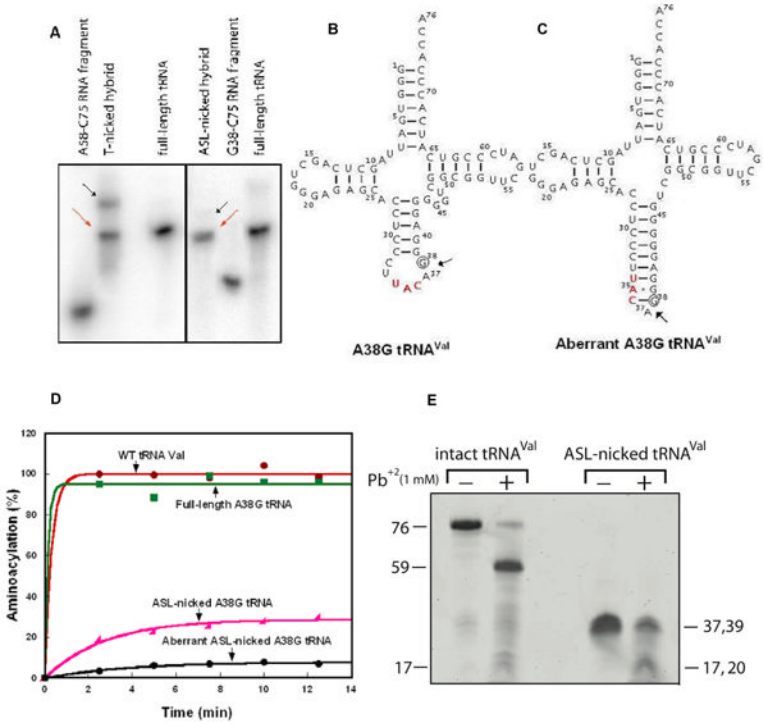

Figure 3.

Characterization of nicked tRNAs. (A) Formation of the T-nicked (left) and ASL-nicked (right) $tRNA_{C75}$ substrates by hybridization of an unlabeled 5′-fragment with a ^{32}P-labeled 3′ fragment. Full-length and intact ^{32}P-$tRNA_{C75}$ was run as a marker. The nicked substrates (indicated by the red arrows) that co-migrated with the intact tRNA marker were isolated from gels and used for analysis of CCA addition, while the aberrant hybridization products that migrated slower than the intact tRNA were marked by black arrows and were not further analyzed for CCA addition. (B) Sequence and cloverleaf structure of the A38G mutant of *E. coli* $tRNA^{Val}$, where the A38G substitution is indicated by a circle. (C) The aberrant structure of the ASL-nicked A38G $tRNA^{Val}$. (D) Aminoacylation of $tRNA^{Val}$ transcripts (2 μM) by purified *E. coli* ValRS (4 μM). (E) Lead cleavage of intact A38G tRNA and the ASL-nicked A38G tRNA analyzed by a 12% denaturing PAGE. The numbers on the sides of the gel indicate the lengths of tRNA or fragments.

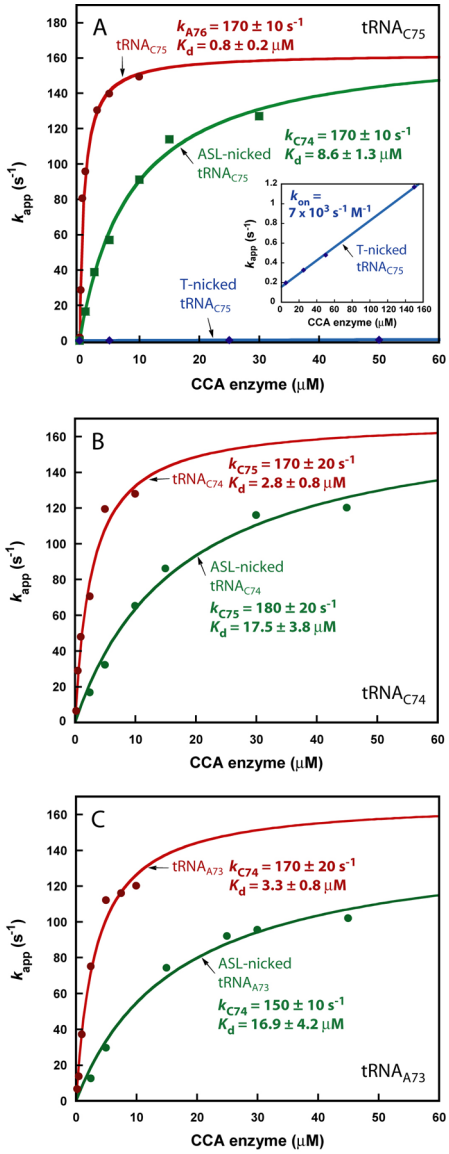

Figure 4.

Kinetics of nicked tRNA. (A) Kinetics of A76 addition to the intact (red), ASL-nicked (green), and T-nicked (blue) $tRNA_{C75}$ as a function of *Ec*CCA concentration. Inset: an expanded view of the k_{app}*vs. Ec*CCA plot for the T-nicked $tRNA_{C75}$. (B) Kinetics of C75 addition to the intact (red) and ASL-nicked (green) $tRNA_{C74}$ as a function of *Ec*CCA concentration. (C) Kinetics of C74 addition to the intact (red) and ASL-nicked (green) $tRNA_{A73}$ as a function of *Ec*CCA concentration. Single turnover rates were monitored by incubating a tRNA substrate with *Ec*CCA, followed by rapid mixing with the correct nucleotide donor.

Table 1

Kinetic[a] parameters of CCA addition[b].

	Intact tRNA			ASL-nicked tRNA			Discrimination
	k_N (s^{-1})	K_d (tRNA, μM)	k_N/K_d ($s^{-1}\mu M^{-1}$)	k_N (s^{-1})	K_d (tRNA, μM)	k_N/K_d ($s^{-1}\mu M^{-1}$)	k_N/K_d (intact)/k_N/K_d (nicked)
A76	170 ± 10	0.8 ± 0.2	212	170 ± 10	8.6 ± 1.3	20	10.6
C75	170 ± 20	2.8 ± 0.8	61	180 ± 20	17.5 ± 3.8	10	6.1
C74	170 ± 20	3.3 ± 0.8	51	150 ± 10	16.9 ± 4.2	8.9	5.7

[a] The reported kinetic K_d (or K_m(sto)) values represent the monomer concentration of *Ec*CCA. In crystal structures of the class I *Af*CCA, the enzyme exists as a dimer and binds two molecules of tRNA or the minihelix domain.[6; 7; 9; 11] In the crystal structure of the class II *Bacillus stearothermophilus* CCA enzyme, the enzyme also exists as a dimer and is modeled to bind two molecules of tRNA.[5; 6]

[b] Values reported are based on experiments performed with pre-incubating *Ec*CCA with a tRNA substrate in one syringe of the rapid quench instrument, followed by rapid mixing with NTP from the other syringe.